IEEE Access
Multidisciplinary | Rapid Review | Open Access Journal

Received April 17, 2018, accepted May 10, 2018, date of publication May 15, 2018, date of current version June 5, 2018.

Digital Object Identifier 10.1109/ACCESS.2018.2836381

Micro Energy Harvester With Dual Electrets on Sandwich Structure Optimized by Air Damping Control for Wireless Sensor Network Application

YULONG ZHANG[1,2], YUSHEN HU[1], XINGE GUO[1], AND FEI WANG[1,2,3], (Senior Member, IEEE)

[1]Department of Electrical and Electronic Engineering, Southern University of Science and Technology, Shenzhen 518055, China
[2]Shenzhen Key Laboratory of 3rd Generation Semiconductor Devices, Southern University of Science and Technology, Shenzhen 518055, China
[3]State Key Lab of Transducer Technology, Shanghai Institute of Microsystem and Information Technology, Chinese Academy of Sciences, Shanghai 200050, China

Corresponding author: Fei Wang (wangf@sustc.edu.cn)

This work was supported in part by the National Natural Science Foundation of China under Grant 51505209, in part by the Shenzhen Science and Technology Innovation Committee under Grants JCYJ20170412154426330 and KQTD2015071710313656, in part by the Guangdong Natural Science Funds for Distinguished Young Scholar under Grant 2016A030306042, and in part by the Guangdong Special Support Program under Grant 2015TQ01X555.

ABSTRACT In this paper, we have designed, fabricated, and characterized a micro-scale electrostatic energy harvester based on microelectromechanical system technology. Sandwich structure with dual electrets was utilized, which can be fully packaged with optimal pressure control to reduce the energy loss from squeeze air damping. With out-of-the-plane gap closing scheme, the energy harvester mainly consists of two variable capacitors, and the overall size of the micro device is about 1.3 cm $\times$ 1.8 cm $\times$ 0.15 cm. With dual electrets, the output power of the device can be increased to 1.5–2 times higher. With low damping effect at packaging pressure of 5 Pa, the normalized power density can be improved by about 2300 times. The device has been used to provide power supply for a battery-free wireless sensor network, and a temperature signal can be posted to internet every 265 s.

INDEX TERMS Energy harvesting, electrets, microelectromechanical systems, damping.

I. INTRODUCTION

Nowadays, more and more wireless electronic devices have been developed with new concept of Internet of Things (IoT) and wireless sensor network (WSN) [1]–[3]. Most of these wireless devices are powered by traditional batteries, which ideally should be replaced by sustainable sources [4]–[6]. For a large scale WSN with distributed sensor nodes, the replacement and disposal of the batteries would be difficult or even infeasible [3]. Recently, micro energy harvesters have attracted much attention as they may be able to provide self-sustainable power supply for the wireless devices with low demand of power consumption, by converting energy sources from environment to electricity. For instance, vibration based micro energy harvesters have been developed with electrostatic [8]–[10], piezoelectric [11]–[13], and electromagnetic principles [14]–[16]. Generally, the electrostatic energy harvester is more compatible with the Si-based fabrication process for the wireless electronic devices.

A typical electrostatic energy harvester consists of a variable capacitor whose capacitance changes according to the vibration source. With a bias voltage [17] or a pre-charged electret layer [18]–[21], current can be induced when one electrode of the capacitor is driven by external excitation. With advanced microelectromechanical system (MEMS) technology, the electrostatic energy harvester takes the advantages of small size, high energy density, and high conversion efficiency [22]–[24].

The capacitance of the device can be described as $C = \varepsilon_0 \varepsilon_r A/d$, where ε_0 and ε_r are the absolute permittivity and relative permittivity, respectively. A is the overlapping area and d is the air gap distance between the two electrodes. As shown in Fig. 1(a) and (b), the device capacitance can be changed when the proof mass vibrates horizontally according to the in-plane excitation [25]–[27]. In Fig. 1a, the overlapping area is changed during the vibration; while the overlapping electrode moves back and forth between the two bottom electrodes in Fig. 1b. With an out-of-the-plane scheme (Fig. 1(c)), the capacitance can also be changed due to the top-down movement of the proof mass. When the electret layer is pre-charged, charges would be induced in the counter

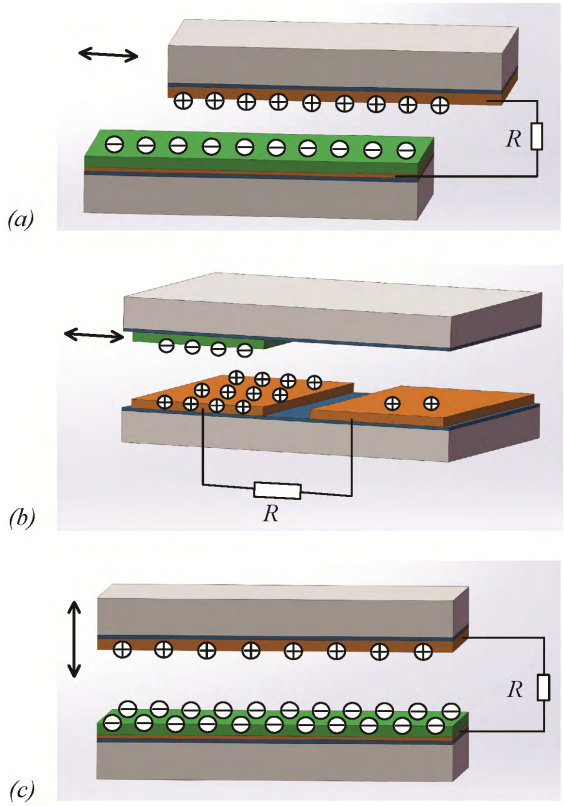

FIGURE 1. Electrostatic energy harvester with variable capacitor, whose capacitance is changed by varying (a) the overlapping area between top and bottom electrodes; (b) overlapping electrode between the left and the right electrodes; (c) gap distance.

electrode; therefore, current is generated from vibration source, which can be used to provide power supply for the external load. Using electret material of PTFE (Polytetrafluoroethylene) and mass made of Tungsten, a cantilever-type energy harvester prototype was fabricated by Boisseau *et al.* [28]. A maximum power of 50 μW was harvested from an active chip size of 4.2 cm^2. In 2014, wafer level fabrication process was developed for MEMS electrostatic energy harvester with the out-of-the-plane gap closing scheme [29]. The device consisted of a four-layers stack, which was packaged as a 1 cm^2 chip using CYTOP (an amorphous perfluoro cyclic polymer from Asahi Glass Group, Japan) both as an electret material and as bonding interfaces between wafers.

The electrostatic devices mentioned above have to face a technical challenge for all the vibration based energy harvesters including piezoelectric and electromagnetic devices, which comes from the energy loss from air damping force. A low overall quality factor of 5 was estimated from the experiment due to the severe squeeze air damping effect from narrow air gap when the proof mass moves close to the electrode [29]. Recently, we have noticed that the air damping effect can be reduced remarkably at low chamber pressure [30], [31]; therefore, the power output of the device can be improved significantly.

In this paper, we propose an electret based micro scale electrostatic energy harvester with sandwich structure, which can be packaged at low air pressure. Compared to the regular linear resonant structure used in the literatures, the sandwich structure provides two stoppers from the top and the bottom caps. With a good control of height, the stoppers can limit the maximum movement amplitude of the proof mass, which results in a broad bandwidth of the harvester. This bandwidth broadening method would benefit the energy harvesting from random vibration sources, which has been partly confirmed by [30] and [31]. Additionally, dual electret layers are used with complementary charges to further improve the power output of the harvester [32], which makes the full use of the two packaging caps and shows more sophisticated effect of the air damping on the device performance, comparing to the single electret layer in [31]. For the first time, we have proposed an electret based energy harvester taking both the advantages of sandwich structure and dual electrets. This manuscript is organized as follow. The design of concept will be firstly described with detailed MEMS fabrication process flow. Characterization of the device is compared between the single device and sandwich structured device. The measurements at various air pressures are conducted to study the damping effect on the device performance. Power output of the devices with single electret and dual electret layers have also been compared. Finally, we have applied the energy harvester for a wireless temperature sensing system.

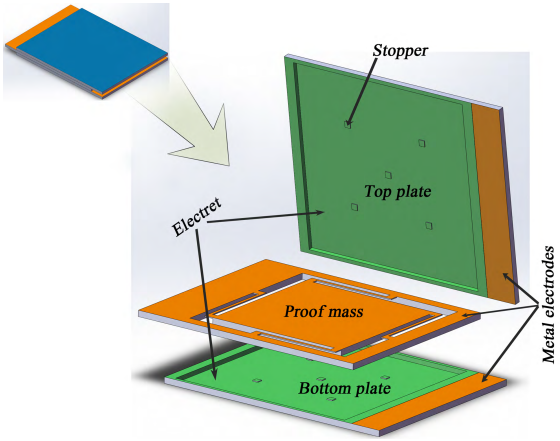

FIGURE 2. 3D schematic of the electrostatic energy harvester with sandwich structure and dual electret layers.

II. DEVICE DESIGN AND FABRICATION

As shown in Fig. 2, the electrostatic energy harvester is designed with sandwich structure which contains three components of a resonant proof mass and two fixed plates. The square proof mass is suspended to a fixed frame through four beams. All the mechanical components are made of silicon. On the top and bottom plates, we have coated electret material of CYTOP on the metal electrode. With different output schemes shown in Fig. 3, we can use this device as a full sandwich device (top and bottom electrodes are connected); a top single device (output with top and central

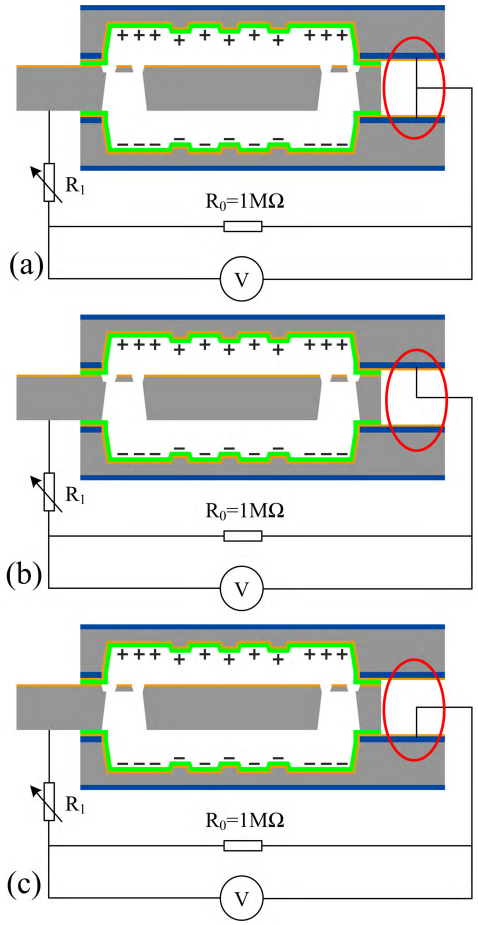

FIGURE 3. Three output schemes naming as (a) full sandwich device; (b) top single device; (c) bottom single device.

electrodes); or a bottom single device (output with bottom and central electrodes).

A. DESIGN OF CONCEPT

The basic principle of the electrostatic energy harvester involves both mechanical and electrical domains. When there is no collision between the proof mass and the plate, we can describe the mechanical performance of the mass-spring-damper system as [33],

$$m(\ddot{y}+\ddot{x})+c\dot{x}+kx+mg-F_{ele}=0 \tag{1}$$

where x and y are the relative displacement of the proof mass and the displacement of the external ambient vibration source, respectively; m is the equivalent mass; g is the gravitational acceleration; k is the stiffness of the spring structure; c and F_{ele} are the damping coefficient and the electrostatic transduction force, respectively. An additional collision force should be added to the model [34]–[36] or the velocity of the proof mass should be tuned [37], when the excitation is high enough to drive the proof mass with vibration amplitude larger than the initial gap. It should be noted that the damping coefficient c in this mechanical model is not constant due to the large movement range of the proof mass. It increases dramatically when the air gap between two electrodes gets narrow [38]. Furthermore, the damping coefficient is also highly dependent on the air pressure. It does not change much when the air pressure is near the atmospheric pressure. When the pressure is pumped down to a pressure level well below, however, the air damping could be significantly reduced, either according to the Energy Transfer Model or the Christian's Model [38]. Thus, it is important to study how packaging pressure affects the performance of the energy harvesting device.

The electric performance of the device depends on the output schemes. For top single device, the governing differential equation can be expressed as,

$$R\frac{dQ_1}{dt}=U-Q_1[\frac{1}{C_1(t)}+\frac{1}{C_2}] \tag{2}$$

where Q_1 is the induced charge on the top electrode; R is the external load resistance; U stands for the surface potential of the pre-charged electret; $C_1(t)$ is the capacitance of the air gap and C_2 is the capacitance of the electret dielectric material. This model can also be applied for the bottom single device; while for the sandwich device, the top and bottom capacitors should be connected in parallel.

TABLE 1. Parameters of the electret-based energy harvester.

Symbol	Parameters	Value
f	resonant frequency	160 Hz
l	beam length	7 mm
w	beam width	200 μm
t	beam thickness	60 μm
m	proof mass	0.1 g
H	silicon wafer thickness	500 μm
g	initial gap	300 μm
h	stopper height	50 μm
d	electret thickness	20 μm
U	surface potential of electret	± 600 V
V	device volume	1.3 cm × 1.8 cm × 0.15 cm

We have used a similar design to our previous work in [31]. As listed in Table 1, the weight of the proof mass is 0.1 g, and each beam has a length of 7 mm, a width of 200 μm, and a thickness of 60 μm. The resonant frequency of this structure is tested as ~160 Hz. The other two fixed plates are designed with the same geometry. Each plate includes a cavity, five stoppers, and a charged electret films. We design the cavity depth of 300 μm to control the initial gap, and the stopper height of 50 μm to prevent the "pull-in" effect of electrostatic force.

B. FABRICATION PROCESS

Fig. 4 shows the detailed fabrication process for the device. Both of the resonant structure and the fixed plates were fabricated in 4-inch silicon wafer using the standard MEMS techniques. As shown in Fig. 4(a), the resonant structure was formed by the double-side lithography (R1 and R3),

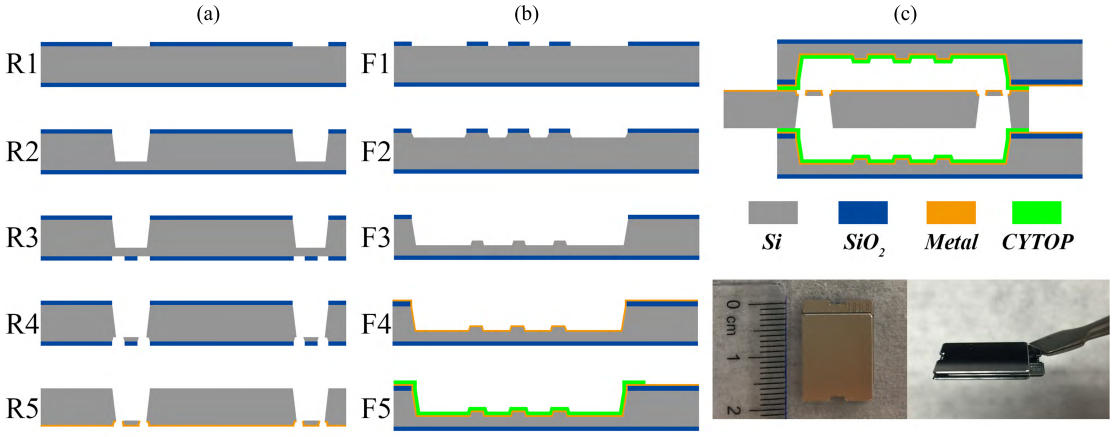

FIGURE 4. Fabrication process flow of the sandwich electrostatic energy harvester with (a) the resonant proof mass; (b) the packaging plate. (c) The device is finally packaged at low pressure with wafer bonding technique. The fabricated device is shown in right-down images with an overall size of 1.3 cm × 1.8 cm × 0.15 cm.

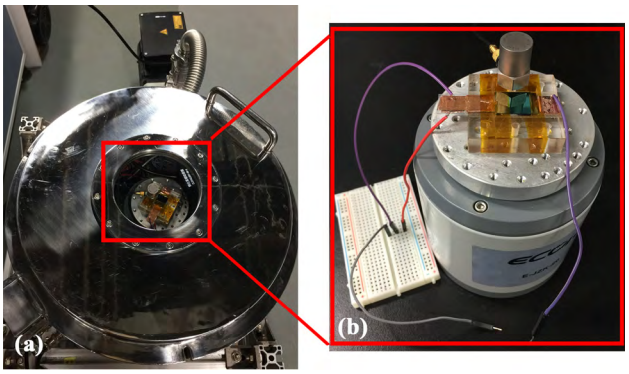

FIGURE 5. (a) Test chamber with a pump to control the air pressure under test; (b) a shaker is used to mimic the external vibration source.

BOE etching for SiO_2 (R1 and R5), KOH etching for Si (R2 and R4), and RIE etching for SiO_2 (R3). As shown in Fig. 4(b), the two fixed plates were formed by lithography (F1), BOE etching for SiO_2 (F1), KOH etching for Si (F2 and F3), RIE etching for SiO_2 (F3). The first KOH etching in F2 was to form the stoppers, and the second in F3 was to form the cavity instead of the conventional spacers to control the initial gap of the device. After the main structure was fabricated, a metal layer of Al (100 nm) was deposited on the surface of the components as the electrodes (R5 and F4). Finally, the CYTOP polymer film (~20 μm) was sprayed on the surface of the cavity (F5) which was an electret material for storing charges and an adhesive layer for low-temperature bonding as well.

After the fabrication, the CYTOP polymer film was charged in a custom-built corona charging setup. The setup consists of a high-voltage probe tip ($V_H = \pm 6$ kV), a mesh grid (Vg = ± 2000 V) and a grounded wafer stage. The top and bottom electret films were opposite charged, and the surface potentials were about ±600 V at 25°C/50%RH, respectively. As shown in Fig. 4(c), the final components were bonded together to form the packaged sandwich device, and the device pictures shown that the volume of the device was about 1.3 cm × 1.8 cm × 0.15 cm.

III. CHARACTERIZATION AND DISCUSSION

The output performance of the electrostatic energy harvester was characterized using a shaker setup to mimic the external vibration source. The shaker is driven by an excitation signal generated from a signal generator (Brüel&Kjær, LAN-XI 3160) and a power amplifier (Brüel&Kjær, 2719), so that the amplitude and the frequency of excitation can be controlled, which could also be monitored by an accelerometer.

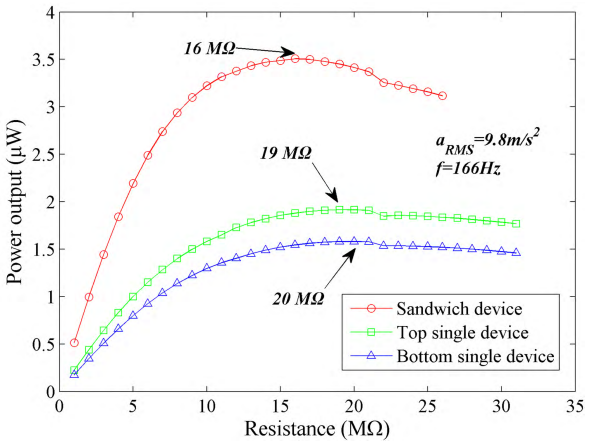

FIGURE 6. The relationship between power outputs and the external load when vibration at frequency of 166 Hz is applied with RMS acceleration amplitude of 9.8 m/s² for the overall sandwich device, the top single device, and the bottom single device, respectively.

It is well known that the power output of energy harvester is dependent on the load resistance. Prior to further investigation on the dual charge and air pressure effects, we have tested the optimal load for each type of the devices, as shown in Fig. 6. When a vibration source with root mean square (RMS)

amplitude of 9.8 m/s^2 is applied at frequency of 166 Hz, the harvested power outputs from sandwich device, top single device and bottom single device are measured with load resistance ranging from 1 to 32 MΩ. A maximum power of 3.5 μW has been harvested from sandwich device with an optimal load of 16 MΩ. Optimal load resistances of 19 MΩ and 20 MΩ are also measured for the top and the bottom single devices, respectively. The optimal resistances will be used for each device during the following measurements unless otherwise mentioned.

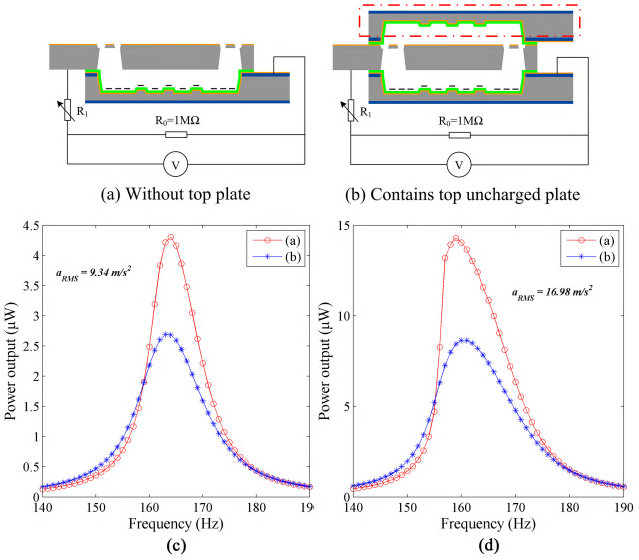

FIGURE 7. Comparison between (a) the conventional unpackaged device and (b) the packaged sandwich structured device. (c) and (d) show the outputs of these devices at the acceleration amplitudes of 9.34 m/s^2 and 16.98 m/s^2, respectively.

A. AIR DAMPING EFFECT FROM SANDWICH STRUCTURE

For practical application, the performance of an unpackaged device could be affected by contaminations from environment. Solid particles may get stuck in the gap between the proof mass and the counter electrode, which would block the movement of the mass. Furthermore, water vapor in humid environment may cause severe decay of the surface charge density in the electret material [18]. Therefore, it is necessary to have a fully packaged design to protect the device from any contamination, as we have previously demonstrated in [29]. In this paper, we have designed the sandwich structure as shown in Fig. 7(b), where the proof mass can be encapsulated by top and bottom plates. Unfortunately, the air damping effect for this sandwich structure could be increased significantly comparing to the open structure with single plate (Fig. 7(a)).

Once the device is fully packaged, a new squeeze air damping (c_2) from the top plate should be added to Eq. (1), which further increases the energy loss and reduces the energy conversion efficiency from mechanical energy to electric energy. Plots in Fig. 7(c)-(d) have shown the power outputs of the device without top plate and the device with sandwich structure, when vibration sources with amplitudes of 9.34 m/s^2 and 16.98 m/s^2 were applied, respectively. With increased vibration amplitude, the power outputs of the devices were also increased. A maximum power of 14.6 μW was harvested from the device without top plate at resonant frequency of 160 Hz, while the output from the device with the top plate was only 8.6 μW under the same excitation. Therefore, about 40% of the power output has been sacrificed for the full package with sandwich structure. This energy loss from the air damping could be alleviated by controlling the chamber pressure to be discussed below.

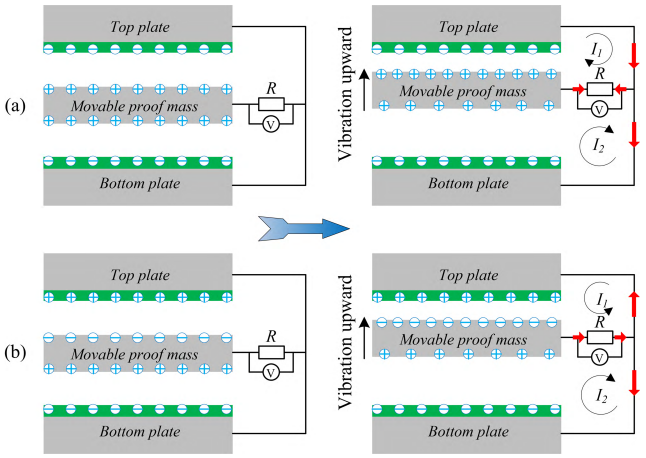

FIGURE 8. The output current flow of the sandwich structured electrostatic energy harvester with dual electrets charged by (a) the same charges; (b) the opposite charges.

B. ENHANCEMENT WITH DUAL ELECTRETS

For the sandwich structured device shown in Fig. 7(b), we can also charge the top plate with the same charge as the bottom plate or with the opposite charge, which result in two different working schemes. The device basically includes two variable capacitors from the electrical point of view. Figure 8(a) shows the scheme when the two plates are charged with the same type of charge, for instance, both negatively charged. When the proof mass vibrates towards the top plate, the amount of the induced positive charge increases on one side while decreases on the other side due to the change of the electrostatic field, which gives two contradictory current flows from the two variable capacitors. When the two plates are charged with the opposite types of charges, as shown in Fig. 8(b), the two induced currents always flow in the same direction, which would enhance the energy harvesting performance under the same vibration source comparing with the single electret devices. Therefore, we will focus on sandwich device with dual electrets charged by opposite types of charges below.

The power output performance was measured with the setup shown in Fig. 3 for the sandwich device, top single device and bottom single device, when vibration sources were applied with frequency ranging from 140 Hz to 180 Hz.

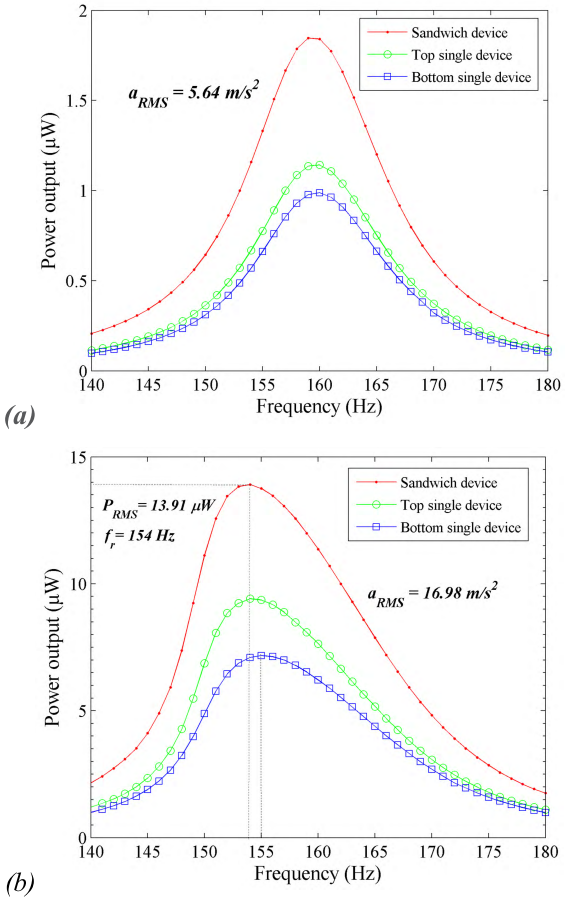

FIGURE 9. Power outputs of the packaged sandwich device with dual charges, the top single device, and the bottom single device under two accelerations of (a) 5.64 m/s^2 and (b) 16.98 m/s^2.

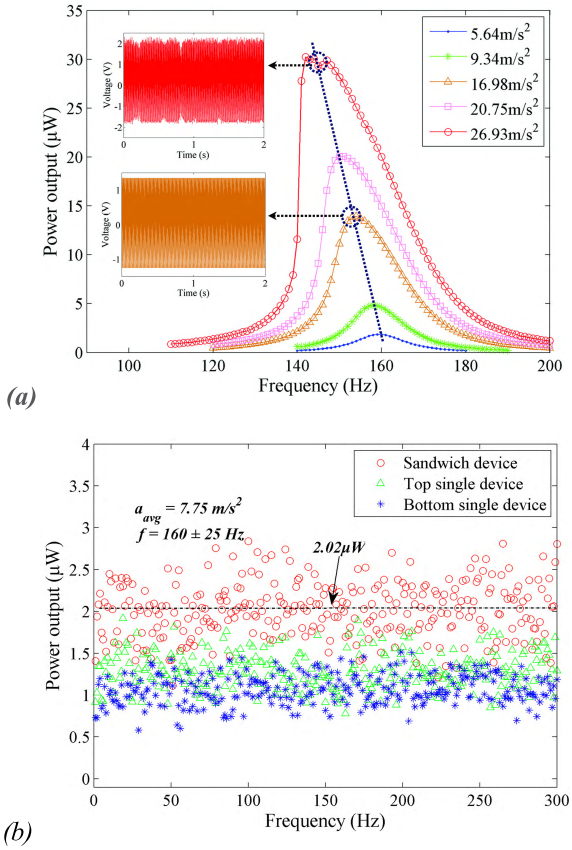

FIGURE 10. (a) Power outputs of the sandwich structured device with dual charges at different accelerations. The inset plots show the typical waveform of output voltage at low excitation (lower) and high excitation amplitude (upper); (b) Comparison of the power outputs of the three devices from random vibration source.

Figure 9(a) and (b) have shown the frequency response results with acceleration amplitudes of 5.64 m/s^2 and 16.98 m/s^2, respectively. Thanks to the addictive effect from two variable capacitors, the sandwich device can always harvest more energy than the top single device and the bottom single device. At vibration frequency of 154 Hz, a maximum power output of 13.91 μW has been harvested from acceleration amplitude of 16.98 m/s^2, which is almost the sum of the power outputs from the two single devices. It should be noted that the resonant frequency of the sandwich structured device is slightly lower than that of the bottom single device due to the increased "softening effect" from the electrostatic force.

The frequency shift from "softening effect" is also seen from Fig. 10(a), where the power outputs of the sandwich structured device are plotted as functions of the vibration frequency at different accelerations. With the acceleration increased from 5.64 m/s^2 to 26.93 m/s^2, the resonant frequency of the device decreases from 159 Hz to 142 Hz. Furthermore, because of the more server squeezed air damping caused by the higher accelerations, broader bandwidth has been observed. The inset plots are the voltage waveforms on a fixed resistance of 1 MΩ at the resonant frequency. When acceleration amplitude of 26.93 m/s^2 is applied, turbulence of output voltage is noticed which indicates that mechanical collision occurs between the proof mass and the fixed plates. Fig. 10(b) shows the harvested power from the sandwich structured device, the top single device, and the bottom single device when random vibration sources were applied for 300 cycles with 2.0 seconds per cycle under the same external random excitation signals. An average power output of 2.02 μW is achieved for sandwich device at RMS acceleration amplitude of 7.75 m/s^2 with a frequency range of 160 ± 25 Hz. As expected, the average power output of the sandwich device is higher than those of the single devices. It should be noted that the efficiency of energy harvesting from random sources is much lower than that from the resonant sinusoidal source. Some methods of intelligent intervention may help to study the vibration pattern, which will be discussed in the future.

C. LOW DAMPING CONTROLLED WITH CHAMBER PRESSURE

To further improve the normalized power density (NPD, defined as harvested power/volume/acceleration^2) of the device, we have tested the devices under low chamber

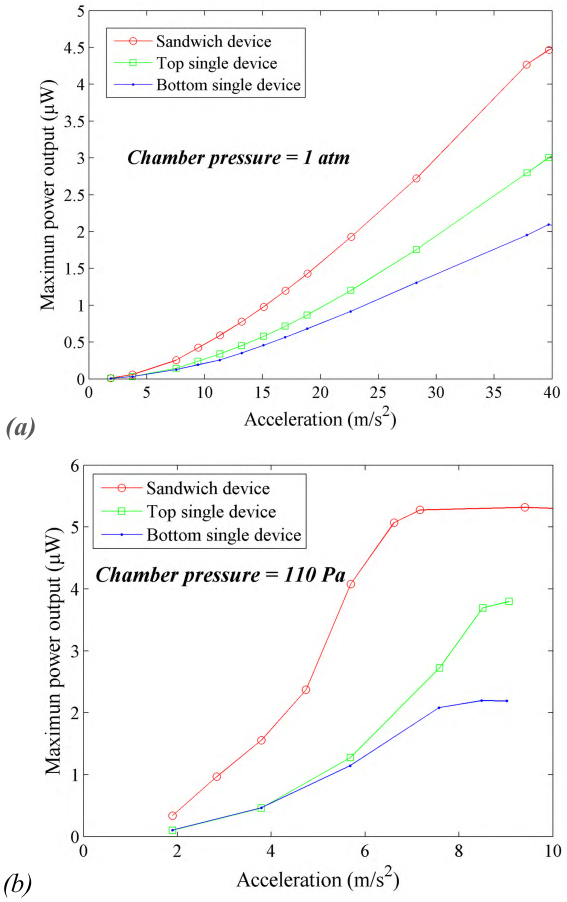

FIGURE 11. Comparison of the output power harvested from the sandwich device, top single device and bottom single device when the devices are tested at chamber pressure of (a) 1 atm; (b) 110 Pa.

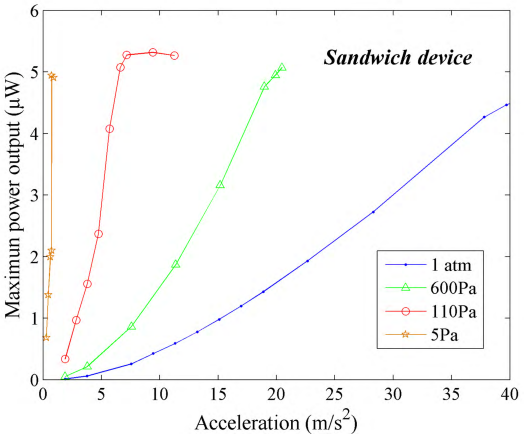

FIGURE 12. The air damping effect for the sandwich device at various chamber pressure from 5 Pa to 1 atm.

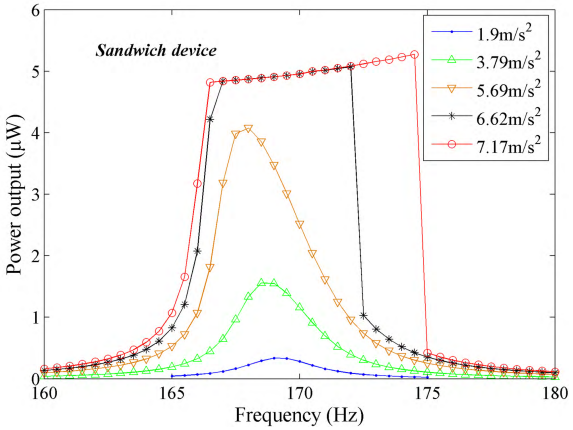

FIGURE 13. The frequency response of the sandwich structured device with different vibration amplitudes at chamber pressure of 110 Pa.

pressure which gives low damping effect and therefore low energy loss during each vibration cycle. Working at atmosphere, all the devices can harvest more energy when the vibration amplitude increases, and maximum power outputs of 4.5 μW, 3.1 μW and 2.2 μW are achieved for sandwich structured device, top single device and bottom single device, respectively, when vibration amplitude of 40 m/s^2 is applied at resonance. It should be noted that the surface potentials of the devices are kept to 200 V during this test. When the chamber pressure is pumped down to 110 Pa, the harvesters can be easily excited at lower vibration amplitude. As shown in Fig. 11(b), the maximum power of each device is slightly higher the value obtained at atmosphere even though more than 5 times lower vibration source is applied. For instance, output power of 5.27 μW can be harvested from low amplitude of 7.16 m/s^2 by the sandwich structured device, thanks to the low damping effect.

Fig. 12 shows the damping effect on the performance of the sandwich structured device with dual electrets when the chamber pressure is pumped down from 1 atm to 5 Pa. The device can always provide maximum power of 4.5-5.3 μW, while the excitation level could be significantly lowered by the damping control. At a low chamber pressure of 5 Pa, the device can be easily excited to the maximum power output at low acceleration amplitude of 0.75 m/s^2 due to the high mechanical Q-factor (Quality factor, defined as the ratio between the total system energy and the average energy loss in one radian at resonant frequency, estimated as ~300). The NPD of the device has been increased by about 2300 times comparing with the atmosphere situation. Another benefit of the damping control is that the bandwidth of the device can also be improved due to the displacement limit of the proof mass by the packaging plates, which has been reported previously [25]. As shown in Fig. 13, the output power of the sandwich structured device saturates at vibration amplitude of 6.62 m/s^2, and a plateau feature has been observed for the frequency response curve. When the excitation amplitude keeps increasing, the output power would not increase because the maximum displacement of the proof mass is limited by the plates. On the other hand, the FWHM (full width at half maximum) bandwidth of the device could be broadened to 9 Hz when the vibration amplitude increases to 7.17 m/s^2.

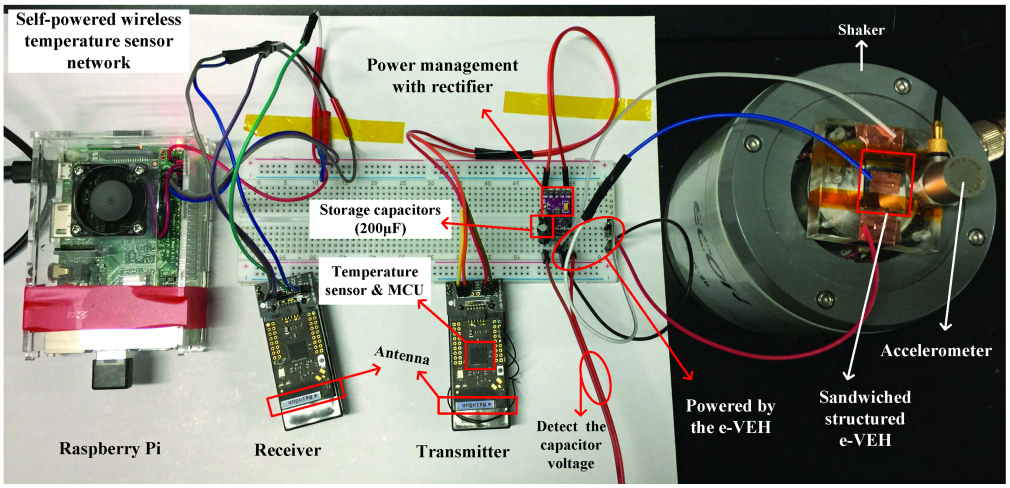

FIGURE 14. The self-powered wireless temperature sensor node, consisting of the power management, micro controller unit (MCU), temperature sensor and radio transmitter. All the components are powered by the sandwich structured electrostatic energy harvester with dual electrets.

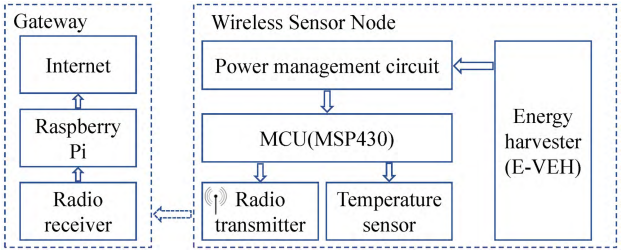

FIGURE 15. Diagram of the self-powered wireless temperature sensor node.

IV. APPLICATION FOR WIRELESS SENSOR

The sandwich structured energy harvester with dual electrets has been used for a self-powered, battery-free wireless temperature sensing network. As shown in Fig. 14, the wireless sensor node consists of energy harvesters, power management circuit, temperature sensor, and radio transmitter, which are fully powered by the electrostatic vibration energy harvester (e-VEH). A storage capacitor of 200 μF is used as a buffer power station, which could be charged by the e-VEH and release the energy for wireless sensing when a trigger signal is received. Fig. 15 shows the diagram of the wireless senor node. More detailed description on the setup of the sensor node can be found in [6] and [31].

A vibration source with amplitude of 17.7 m/s^2 has been applied to mimic the vibrations from environment. Fig. 16(a) shows the voltage on the storage capacitor during the charging and energy releasing for temperature sensing, and a demo of the wireless sensing application can be more clearly seen from the Supplementary Video. After a cold start of about 870 s to charge the capacitor to a voltage of 4.05 V, a trigger signal is sent to the MCU which can release part of the storage energy to acquire and send out a temperature signal through the transmitter. Afterwards, the wireless signal can be consecutively sent out every 265 s. The voltage of the capacitor drops to 3.05 V after sending a temperature signal.

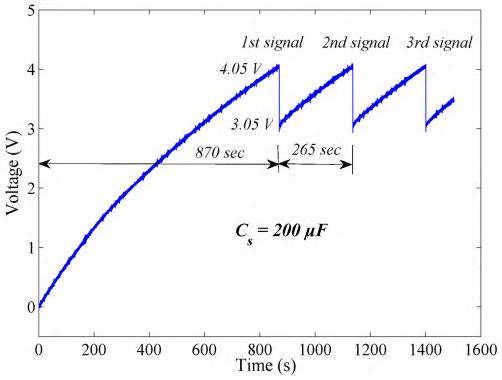

(a)

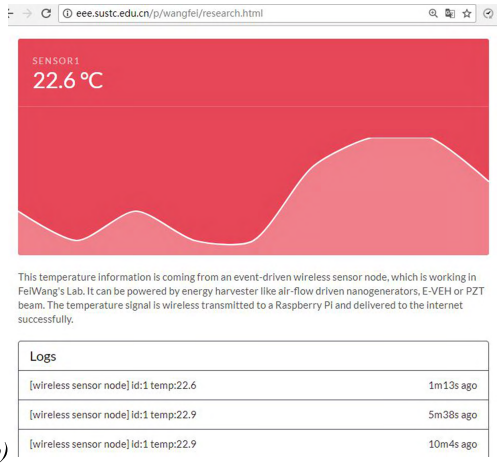

(b)

FIGURE 16. (a) Voltage on the storage capacitor of 200 μF during the charging and energy releasing; (b) After a cold start of 870 s, the wireless temperature signal can be transmitted every 265 s, which would be further posted to the internet.

The overall energy consumed for each cycle can be calculated as,

$$E = \frac{1}{2}C\left(V_1^2 - V_2^2\right) = \frac{1}{2}\times 200\times\left(4.05^2 - 3.05^2\right) = 710\mu J \quad (3)$$

Based on that, the average power for charging the capacitor can be estimated as $710/265 = 2.68\ \mu$W. As shown in Fig. 15(b), the real-time temperature information is posted on the webpage of our group, which could be accessed anywhere with a smart phone. This experiment demonstrates a promising prototype for the self-powered wireless sensor networks, with a potential application for the remote temperature sensing for many scenarios. Environment surveillance on highway road or body temperature monitoring for animals in a farm could be good examples as the sensing signal only need to be acquired from time to time when required (for instance, once half a hour) without a continuous data processing.

V. CONCLUSION

In this paper, we have proposed an optimization method for micro electrostatic energy harvester using dual electrets on sandwich structure packaged by low air damping chamber. The effects from sandwich structure, dual electrets and packaging pressure on the power output of the energy harvester have been investigated with experimental details. Maximum power output up to 30 μW has been harvested from vibration amplitude of 26.93 m/s^2 at 142 Hz. The harvested power from random vibration has also been improved with the dual electrets on sandwich structure. With the low air damping, the NPD of the device can be increased by 2300 times. We have applied the sandwich structured harvester for wireless temperature sensing network, which proves very promising potential for practical application.

REFERENCES

[1] S. Sudevalayam and P. Kulkarni, "Energy harvesting sensor nodes: Survey and implications," *IEEE Commun. Surveys Tuts.*, vol. 13, no. 3, pp. 443–461, 3rd Quart., 2010.

[2] C. Li, Y. Fu, Z. Liu, X.-Y. Liu, W. Wu, and L. Xiong, "Spectrum trading for energy-harvesting-enabled Internet of Things in harsh environments," *IEEE Access*, vol. 6, pp. 16712–16726, 2018, doi: 10.1109/ACCESS.2018.2808291.

[3] O. Cetinkaya and O. B. Akan, "Electric-field energy harvesting from lighting elements for battery-less Internet of things," *IEEE Access*, vol. 5, pp. 7423–7434, 2017, doi: 10.1109/ACCESS.2017.2690968.

[4] B. E. White, Jr., "Energy-harvesting devices: Beyond the battery," *Nature Nanotechnol.*, vol. 3, no. 2, pp. 71–72, 2008.

[5] X. Gu *et al.*, "Hybridization of integrated microwave and mechanical power harvester," *IEEE Access*, vol. 6, pp. 13921–13930, 2018, doi: 10.1109/ACCESS.2018.2814003.

[6] Y. Wu, Y. Hu, Z. Huang, C. Lee, and F. Wang, "Electret-material enhanced triboelectric energy harvesting from air flow for self-powered wireless temperature sensor network," *Sens. Actuators A, Phys.*, vol. 271, pp. 364–372, Mar. 2018.

[7] P. D. Mitcheson, E. M. Yeatman, G. K. Rao, A. S. Holmes, and T. C. Green, "Energy harvesting from human and machine motion for wireless electronic devices," *Proc. IEEE*, vol. 96, no. 9, pp. 1457–1486, Sep. 2008.

[8] Y. Suzuki, "Recent progress in MEMS electret generator for energy harvesting," *IEEJ Trans. Elect. Electron. Eng.*, vol. 6, no. 2, pp. 101–111, 2011.

[9] H. W. Lo and Y. C. Tai, "Parylene-based electret power generators," *J. Micromech. Microeng.*, vol. 18, no. 10, p. 104006, Sep. 2008, doi: 10.1088/0960-1317/18/10/104006.

[10] A. Crovetto, F. Wang, and O. Hansen, "An electret-based energy harvesting device with a wafer-level fabrication process," *J. Micromech. Microeng.*, vol. 23, no. 11, p. 114010, Oct. 2013.

[11] K. A. Cook-Chennault, N. Thambi, and A. M. Sastry, "Powering MEMS portable devices—A review of non-regenerative and regenerative power supply systems with special emphasis on piezoelectric energy harvesting systems," *Smart Mater. Struct.*, vol. 17, no. 4, p. 043001, Jun. 2008.

[12] S. Li *et al.*, "Bi-resonant structure with piezoelectric PVDF films for energy harvesting from random vibration sources at low frequency," *Sens. Actuators A, Phys.*, vol. 247, pp. 547–554, Aug. 2016.

[13] L. Gu and C. Livermore, "Passive self-tuning energy harvester for extracting energy from rotational motion," *Appl. Phys. Lett.*, vol. 97, no. 8, p. 081904, Aug. 2010.

[14] S. P. Beeby *et al*, "A micro electromagnetic generator for vibration energy harvesting," *J. Micromech. Microeng.*, vol. 17, no. 7, pp. 1257–1265, Jun. 2007.

[15] Q. Zhang and E. S. Kim, "Vibration energy harvesting based on magnet and coil arrays for watt-level handheld power source," *Proc. IEEE*, vol. 102, no. 11, pp. 1747–1761, Nov. 2014.

[16] B. Yang and C. Lee, "Non-resonant electromagnetic wideband energy harvesting mechanism for low frequency vibrations," *Microsyst. Technol.*, vol. 16, no. 6, pp. 961–966, 2010.

[17] A. M. Paracha, P. Basset, D. Galayko, F. Marty, and T. Bourouina, "A silicon MEMS DC/DC converter for autonomous vibration-to-electrical-energy scavenger," *IEEE Electron Device Lett.*, vol. 30, no. 5, pp. 481–483, May 2009.

[18] H. Asanuma, H. Oguchi, M. Hara, R. Yoshida, and H. Kuwano, "Ferroelectric dipole electrets for output power enhancement in electrostatic vibration energy harvesters," *Appl. Phys. Lett.*, vol. 103, no. 16, p. 162901, Oct. 2013.

[19] F. Wang, C. Bertelsen, G. Skands, T. Pedersen, and O. Hansen, "Reactive ion etching of polymer materials for an energy harvesting device," *Microelectron. Eng.*, vol. 97, pp. 227–230, Sep. 2012.

[20] M. Renaud *et al.*, "A high performance electrostatic MEMS vibration energy harvester with corrugated inorganic SiO_2-Si_3N_4 electret," in *Proc. 17th Int. Conf. Solid-State Sens., Actuators Microsyst.*, Barcelona, Spain, Jun. 2013, pp. 693–696.

[21] Y. Xu *et al.*, "Spray coating of polymer electret with polystyrene nanoparticles for electrostatic energy harvesting," *IET Micro Nano Lett.*, vol. 11, no. 10, pp. 640–644, 2016.

[22] Y. Chiu and Y.-C. Lee, "Flat and robust out-of-plane vibrational electret energy harvester," *J. Micromech. Microeng.*, vol. 23, no. 1, p. 015012, Dec. 2013.

[23] K. Tao, L. Tang, J. Wu, S. W. Lye, H. Chang, and J. Miao, "Investigation of multimodal electret-based MEMS energy harvester with impact-induced nonlinearity," *J. Microelectromech. Syst.*, vol. 27, no. 2, pp. 276–288, Apr. 2018.

[24] F. Cottone, P. Basset, R. Guilllemet, D. Galayko, F. Marty, and T. Bourouina, "Non-linear MEMS electrostatic kinetic energy harvester with a tunable multistable potential for stochastic vibrations," in *Proc. 17th Int. Conf. Solid-State Sens., Actuators Microsyst.*, Barcelona, Spain, Jun. 2013, pp. 1336–1339.

[25] F. Wang and O. Hansen, "Invisible surface charge pattern on inorganic electrets," *IEEE Electron Device Lett.*, vol. 34, no. 8, pp. 1047–1049, Aug. 2013.

[26] Y. Suzuki, D. Miki, M. Edamoto, and M. Honzumi, "A MEMS electret generator with electrostatic levitation for vibration-driven energy-harvesting applications," *J. Micromech. Microeng.*, vol. 20, no. 10, p. 104002, 2010.

[27] Y. Minakawa, R. Chen, and Y. Suzuki, "X-shaped-spring enhanced MEMS electret generator for energy harvesting," in *Proc. 17th Int. Conf. Solid-State Sens., Actuators Microsyst.*, Barcelona, Spain, Jun. 2013, pp. 2241–2244.

[28] S. Boisseau, G. Despesse, T. Ricart, E. Defay, and A. Sylvestre, "Cantilever-based electret energy harvesters," *Smart Mater. Struct.*, vol. 20, no. 10, p. 105013, Aug. 2011.

[29] F. Wang and O. Hansen, "Electrostatic energy harvesting device with out-of-the-plane gap closing scheme," *Sens. Actuators A, Phys.*, vol. 211, pp. 131–137, May 2014.

[30] Y. Zhang, Y. Hu, S. Chen, Z. Peng, X. Li, and F. Wang, "Electret based micro energy harvesting device with both broad bandwidth and high power density from optimal air damping," in *Proc. 19th Int. Conf. Solid-State Sens., Actuators Microsyst.*, Kaohsiung, Taiwan, Jun. 2017, pp. 355–358.

[31] Y. Zhang, T. Wang, A. Luo, Y. Hu, X. Li, and F. Wang, "Micro electrostatic energy harvester with both broad bandwidth and high normalized power density," *Appl. Energy*, vol. 212, pp. 362–371, Feb. 2018.

[32] K. Tao, J. Wu, L. Tang, L. Hu, S. W. Lye, and J. Miao, "Enhanced electrostatic vibrational energy harvesting using integrated opposite-charged electrets," *J. Micromech. Microeng.*, vol. 27, no. 4, p. 044002, Mar. 2017.
[33] A. Crovetto, F. Wang, and O. Hansen, "Modeling and optimization of an electrostatic energy harvesting device," *J. Microelectromech. Syst.*, vol. 23, no. 5, pp. 1141–1155, Oct. 2014.
[34] T. Takahashi, M. Suzuki, T. Nishida, Y. Yoshikawa, and S. Aoyagi, "Vertical capacitive energy harvester positively using contact between proof mass and electret plate—Stiffness matching by spring support of plate and stiction prevention by stopper mechanism," in *Proc. 28th IEEE Int. Conf. Micro Electro Mech. Syst.*, Estoril, Portugal, Jan. 2015, pp. 1145–1148.
[35] Y. Zhang *et al.*, "Electrostatic energy harvesting device with dual resonant structure for wideband random vibration sources at low frequency," *Rev. Sci. Instrum.*, vol. 87, no. 12, p. 125001, Dec. 2016.
[36] H. Asanuma, M. Hara, H. Oguchi, and H. Kuwano, "Nonlinear restoring force of spring with stopper for ferroelectric dipole electret-based electrostatic vibration energy harvesters," *AIP Adv.*, vol. 6, no. 7, p. 075206, Jul. 2016.
[37] S. Li, Z. Peng, A. Zhang, and F. Wang, "Dual resonant structure for energy harvesting from random vibration sources at low frequency," *AIP Adv.*, vol. 6, no. 1, p. 015019, Jan. 2016.
[38] M. Bao, *Analysis and Design Principles of MEMS Devices*. Amsterdam, The Netherlands, Elsevier, 2005, pp. 115–173.

YULONG ZHANG received the B.S. degree in physics from Taiyuan Normal University, Taiyuan, China, in 2011, and the M.S. degree in physical electronics from the Xi'an University of Technology, Xi'an, China, in 2014.

From 2014 to 2015, he was a Research and Development Engineer with Shenzhen Selen Science & Technology Co. Ltd., Shenzhen, China. Since 2015, he has been a Research Assistant with the Department of Electrical and Electronic Engineering, Southern University of Science and Technology, Shenzhen. His current research interests include the micro energy harvester, microelectromechanical system techniques, and preparation of nano-sized semiconductor materials.

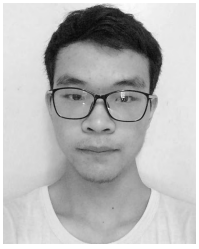

YUSHEN HU is currently pursuing the bachelor's degree with the Department of Electrical and Electronic Engineering, Southern University of Science and Technology, China. His current research interests include circuit design and test for energy harvesters and self-powered wireless sensor network system.

XINGE GUO is currently pursuing the bachelor's degree with the Department of Electrical and Electronic Engineering, Southern University of Science and Technology, China. His current research interests include mechanical design and test for energy harvesters.

FEI WANG (S'06–M'09–SM'12) received the B.S. degree in mechanical engineering from the University of Science and Technology of China, Hefei, China, in 2003, and the Ph.D. degree in microelectronics from the Shanghai Institute of Microsystem and Information Technology, Chinese Academy of Science, Shanghai, China, in 2008.

He was a Post-Doctoral Researcher with the Department of Micro- and Nano-technology, Technical University of Denmark, where he had been an Assistant Professor since 2010. Since 2013, he has been an Associate Professor with the Department of Electrical and Electronic Engineering, Southern University of Science and Technology, China. His current research interests include micro energy harvesting, microelectromechanical system and NEMS sensors, and semiconductor testing.

Dr. Wang served as a TPC Member for the 19th International Conference on Solid-State Sensors, Actuators and Microsystems (Transducers 2017), the 13th International Conference on Nano/Micro Engineered and Molecular Systems (NEMS 2018), and the International Conference on Manipulation, Manufacturing and Measurement on the Nanoscale (IEEE 3M-NANO) from 2014 to 2017.